Interactions of Plasminogen Activator Inhibitor-1 with Vitronectin Involve an Extensive Binding Surface and Induce Mutual Conformational Rearrangements†

Grant E. Blouse,‡,§ Daniel M. Dupont,‡ Christine R. Schar,|| Jan K. Jensen,‡ Kenneth H. Minor,|| John Y. Anagli,§ Henrik Gårdsvoll,⊥ Michael Ploug,⊥ Cynthia B. Peterson,|| and Peter A. Andreasen*,‡

Laboratory of Cellular Protein Science, Department of Molecular Biology, University of Aarhus, Gustav Wieds Vej 10C, DK-8000 Århus C, Denmark, Department of Biochemistry, Cellular, and Molecular Biology and Center of Excellence in Structural Biology, University of Tennessee, Knoxville, Tennessee 37996, Finsen Laboratory 3735, Rigshospitalet, Copenhagen Biocenter, Ole Maaløes Vej 5, DK-2200 Copenhagen N, Denmark, Department of Pathology, Henry Ford Health System, Detroit, Michigan 48202, and Department of Pharmacology, Wayne State University School of Medicine, Detroit, Michigan 48201

Received September 7, 2008; Revised Manuscript Received December 9, 2008

ABSTRACT: In order to explore early events during the association of plasminogen activator inhibitor-1 (PAI-1) with its cofactor vitronectin, we have applied a robust strategy that combines protein engineering, fluorescence spectroscopy, and rapid reaction kinetics. Fluorescence stopped-flow experiments designed to monitor the rapid association of PAI-1 with vitronectin indicate a fast, concentration-dependent, biphasic binding of PAI-1 to native vitronectin but only a monophasic association with the somatomedin B (SMB) domain, suggesting that multiple phases of the binding interaction occur only when full-length vitronectin is present. Nonetheless, in all cases, the initial fast interaction is followed by slower fluorescence changes attributed to a conformational change in PAI-1. Complementary experiments using an engineered, fluorescently silent PAI-1 with non-natural amino acids showed that concomitant structural changes occur as well in native vitronectin. Furthermore, we have measured the effect of vitronectin on the rate of insertion of the reactive center loop into β-sheet A of PAI-1 during reaction with target proteases. With a variety of PAI-1 variants, we observe that both full-length vitronectin and the SMB domain have protease-specific effects on the rate of loop insertion but that the two exhibit clearly different effects. These results support a model for PAI-1 binding to vitronectin in which the interaction surface extends beyond the region of PAI-1 occupied by the SMB domain. In support of this model are recent results that define a PAI-1-binding site on vitronectin that lies outside the somatomedin B domain (Schar, C. R., Blouse, G. E., Minor, K. H., and Peterson, C. B. (2008) *J. Biol. Chem. 283*, 10297−10309) and the complementary site on PAI-1 (Schar, C. R., Jensen, J. K., Christensen, A., Blouse, G. E., Andreasen, P. A., and Peterson, C. B. (2008) *J. Biol. Chem. 283*, 28487−28496).

Plasminogen activator inhibitor-1 (PAI-1),[1] the primary inhibitor of the tissue-type (tPA) and urokinase-type (uPA) plasminogen activators, is the foremost regulator of both fibrinolysis and pericellular plasminogen activation, thus making it a particularly attractive target for therapeutic intervention in cardiovascular disease and cancer (*1*−*3*). Largely, the role of PAI-1 has been viewed in light of its function as a "classic" suicide-substrate inhibitor of the serpin fold (*4*). However, the continuing identification of new and multifunctional serpins in a variety of organisms attests to the critical biological roles and evolutionary adaptability of this gene family to assume key nonantiproteolytic functions (*5*−*7*).

An important physiological partner of PAI-1 *in vivo* is the M_r ~70000 adhesive glycoprotein, vitronectin (*8*−*10*). Interactions between these two proteins exhibit high affinity (K_d ~0.5 nM) and are mediated via contacts between the amino-terminal somatomedin B (SMB) domain of vitronectin and the flexible joint region of PAI-1 in the vicinity of α-helices D, E, and F (*11*−*14*). Given that the circulating concentration of vitronectin is in the near micromolar range, while PAI-1 is present at nanomolar concentrations, active PAI-1 is typically found in a tight complex with vitronectin.

† This work was supported by the European Union FP6 Contract LSHC-CT-2003-503297, the Cancer Degradome Project, Danish Cancer Society, Danish Cancer Research Foundation, and the Novo Nordisk Foundation (to P.A.A.), Grant HF 95092534 from the Danish Heart Association (to G.E.B.), Grant HL54930 from the Heart, Lung, and Blood Institute at the National Institutes of Health (awarded to Joseph D. Shore and posthumously transferred to J.Y.A.), and Grant HL50676 from the Heart, Lung, and Blood Institute at the National Institutes of Health (to C.B.P.) D.M.D. is a recipient of a Ph.D. stipend from the Interdisciplinary Nanoscience Center at the University of Aarhus.

* Address correspondence to this author. Tel: +45 89 42 5080. Fax: +45 8612 3178. E-mail: PA@mb.au.dk.

‡ University of Aarhus.

§ Henry Ford Health System and Wayne State University School of Medicine.

|| University of Tennessee.

⊥ Copenhagen Biocenter.

[1] Abbreviations: PAI-1, plasminogen activator inhibitor type 1; tPA, tissue-type plasminogen activator; uPA, urokinase plasminogen activator; ECM, extracellular matrix; SMB, somatomedin B domain of vitronectin; nVN, native, monomeric vitronectin; rSMB, recombinant SMB domain from *Pichia pastoris*; SDS−PAGE, sodium dodecyl sulfate−polyacrylamide gel electrophoresis; P1−P1′ refer to Schecter and Berger nomenclature for the reactive center loop residues of PAI-1, where P1, P2, P3, P4,... and P1′, P2′, P3′, P4′,... denote those residues on the amino-terminal and carboxyl sides of the scissile bond, respectively; 4-FTrp, the 4-fluorotryptophan analogue of tryptophan; 4-FTrp PAI-1, PAI-1 incorporated with the 4-fluorotryptophan analogue; NBD, *N*,*N*′-dimethyl-*N*-acetyl-*N*′-methyl(7-nitrobenz-2-oxa-1,3-diazol-4-yl)ethylenediamine; k_{assoc}, second-order association rate constant for complex formation; k_{lim}, limiting rate constant; HEPES, 4-(2-hydroxyethyl)piperazine-1-ethansulfonic acid; EDTA, ethylenediaminetetraacetic acid.

10.1021/bi8017015 CCC: $40.75
Published on Web 02/04/2009

As a binding partner for PAI-1, vitronectin has been reported to localize the serpin to fibrin clots (*15*), cause accumulation of PAI-1 in the extracellular matrix (ECM) (*16*), and confer on PAI-1 the ability to inhibit other proteases of the coagulation cascade (*17, 18*). Vitronectin delays the conversion of PAI-1 to the inactive, so-called "latent" state. On the other hand, latent PAI-1 has a much lower affinity for vitronectin than the active form (for a review, see Dupont et al. (*19*)). Vitronectin readily associates with cell-surface receptors, including integrins, uPAR, and elements of the ECM (*20*−*25*). PAI-1 and vitronectin are colocalized in extracellular compartments during tumor development, angiogenesis, inflammation, and necrosis (*26*−*28*). Vitronectin that has been incorporated into the ECM assumes an altered, oligomeric state that is structurally distinct from that of the corresponding native circulating plasma vitronectin (*29*). Vitronectin incorporated into the ECM adopts cell-binding functions.

The range of effects that vitronectin has on PAI-1 localization and activity underscores the relevance of evaluating the mechanism and modes of binding that exist for these two partner proteins. For some time it has been speculated that the binding of PAI-1 and other ligands to vitronectin may initiate its transformation to the altered, ECM-associated form (*30, 31*). However, direct evidence for a PAI-1 induced conformational change in vitronectin has been scarce. Some studies have suggested that PAI-1 may interact with regions of vitronectin that are outside of the well-described binding surface in the SMB domain (*32*−*34*), consequently modulating this conformational effect (*15, 35, 36*). Conclusive evidence for a second binding site for vitronectin and PAI-1 has come recently from our work characterizing a deletion mutant of vitronectin that lacks the somatomedin B domain, yet retains PAI-1 binding (*37*). Also, the complementary site on PAI-1 has been mapped using a battery of point mutants and shown to comprise a region separate from the somatomedin B binding area at the distal end of α-helices D and E (*38*). The present work was devised to explore the early molecular events that characterize the interaction of PAI-1 and native monomeric vitronectin, to address how this interaction influences reactions with target proteases, and to test directly whether PAI-1 elicits a structural transition in vitronectin. In order to resolve these key issues, we have taken an approach that merges the techniques of fluorescence spectroscopy and rapid reaction kinetics to define the nature and stoichiometry of intermolecular interactions between PAI-1 and monomeric vitronectin.

EXPERIMENTAL PROCEDURES

Materials and Reagents. Unless otherwise indicated all spectral and kinetic measurements were performed at pH 7.4 and 25 °C in a HEPES/NaCl reaction buffer of 30 mM HEPES, 0.135 M NaCl, and 1 mM EDTA and containing 0.1% polyethylene glycol 8000 for reduction of protein adsorption. Chromatography materials were obtained from Amersham Pharmacia Biotech (Uppsala, Sweden). Oligonucleotides were synthesized and HPLC purified by Cruachem (Aston, PA) or DNA Technology (Århus, Denmark). All other reagents were of analytical reagent grade or better and were obtained from Sigma.

Recombinant PAI-1 Mutagenesis, Expression, and Purification. We will refer to amino acid residues in PAI-1 by the numbering system of Andreasen et al., starting at Ser^1-Ala^2-Val^3 (*39*). Construction of the pET-24d vector (Novagen) encoding a non-His_6-tag recombinant human PAI-1 has been described (*40*). The S121C mutation was engineered by the established site-directed mutagenesis techniques of Kunkel (*41, 42*). Preparation of the E352A/E353A/S340C PAI-1 exosite mutant at P4′ and P5′ has been described previously (*43*). Mutant and wild-type non-His_6-tag PAI-1 were expressed in the *Escherichia coli* strain BL21(DE3)pLysS and purified as described (*40*). All other recombinant PAI-1 variants including S340C, K325A/S340C, Stab/S340C, R117E/R120E/S340C, and Stab/R117E/R120E/S340C were constructed in the pT7-PL vector, expressed with an N-terminal His_6 tag, and purified from *E. coli* expression cultures as described previously (*44*). The stable, active PAI-1 variant (Stab) carries the four amino acid substitutions described by Berkenpas et al. (*45*). DNA sequencing of the full-length PAI-1 gene confirmed all mutations. All final preparations were shown to be >98% active by SDS−PAGE analysis (*40, 46*). PAI-1 protein concentrations were measured at 280 nm, using a M_r of 43000 and an extinction coefficient of 0.93 mL mg^{-1} cm^{-1} for wild-type PAI-1 and variants (*47*).

Fluorescence Labeling of Recombinant PAI-1. Labeling of the S121C PAI-1 variants was performed with *N*,*N*′-dimethyl-*N*-acetyl-*N*′-methyl(7-nitrobenz-2-oxa-1,3-diazol-4-yl)ethylenediamine (IANBD amide; Molecular Probes) to create the fluorescently labeled variant, $PAI\text{-}1_{121\text{-}NBD}$, essentially as described (*48*). Labeling of the P9-Cys residue in PAI-1 (S340C) and the above-described S340C variants was carried out with *N*-((2-(iodoacetoxy)ethyl)-*N*-methyl)-amino-7-nitrobenz-2-oxa-1,3-diazole (IANBD ester; Molecular Probes) in the same manner as the labeling of S121C (*48*). The typical labeling efficiencies were above 0.8 mol of probe/mol of PAI-1, irrespective of the PAI-1 variant. Incorporation of the fluorescent probes at these positions on PAI-1 was shown previously to have no adverse effects on PAI-1 activity (*49, 50*). Latent PAI-1, which typically accumulated during the labeling reaction, was subsequently removed by affinity chromatography on immobilized β-anhydrotrypsin as described (*46*). Labeled PAI-1 protein concentrations were determined as described above or measured by the Bradford dye-binding assay (Bio-Rad) using wild-type PAI-1 of known concentration as the standard (*51*).

Incorporation of 4-Fluorotryptophan (4-FTrp) into PAI-1. Biosynthetic incorporation of the tryptophan analogue, 4-FTrp, was achieved by recombinant expression in the *E. coli* tryptophan auxotroph strain W3110TrpA33(DE3)pLysS using the one-step analogue incorporation method described previously (*52*). The efficiency of 4-fluorotryptophan substitution into PAI-1 was determined by MALDI-TOF mass spectrometry as described (*52*) and indicated that only one major peak was present representing a PAI-1 molecule with a mass of 42700 Da. This 67 Da increase in mass compared to that of the wild-type PAI-1 control (42630 Da) was within the experimental error of the theoretical 72 Da increase in mass expected for the substitution of all four tryptophans with 4-fluorotryptophan and thus is consistent with all four residues being completely replaced. All final unlabeled and

labeled preparations were shown to be >98% active by SDS−PAGE analysis (*40, 46*). Concentrations were determined by the Bradford dye-binding assay (Bio-Rad) using wild-type PAI-1 of known concentration as the standard (*51*).

Human Vitronectin Proteins. Native monomeric vitronectin was purified from human plasma as described previously (*53, 54*). Purified monomeric vitronectin was stored at 4 °C as an ammonium sulfate pellet and resuspended in HEPES/NaCl reaction buffer immediately before use. Gel filtration chromatography on a 20 mL Superdex S-200 column using a mobile phase of PBS (0.038 M Na_2HPO_4, 0.011 M NaH_2PO_4, 0.145 M NaCl) at pH 7.4 confirmed that the monomeric nature of the preparation was retained. Expression and purification of the recombinant somatomedin B domain of vitronectin containing residues 1−47 and a C-terminal His_6 tag in a *Pichia pastoris* expression vector are described elsewhere (*55*). Preparation of the somatomedin B domain from native plasma vitronectin by cyanogen bromide digestion has been described previously (*56*).

Proteases. Human recombinant tPA (Activase) was provided by Genentech Inc. (San Francisco, CA). The bulk drug tPA preparation is largely composed of the single chain form and was subsequently converted to the two-chain form by continuous fluxing of the tPA preparation through a 1 mL plasmin Sepharose column as previously described (*46*). Human recombinant high molecular weight two-chain uPA was provided by Abbott Laboratories (Chicago, IL) or purchased from Wakamoto Pharmaceutical Co. (Tokyo, Japan). Protease concentrations were determined from the absorbance at 280 nm using extinction coefficients of 1.93 and 1.36 mL mg^{-1} cm^{-1} and M_r values of 63500 and 54000 for tPA and uPA, respectively.

Fluorescence Emission Spectroscopy. Emission spectra from equilibrium binding reactions between PAI-$1_{121\text{-NBD}}$ or 4-FTrp PAI-1 and vitronectin proteins were carried out with Varian Cary Eclipse or SPEX-3 spectrofluorometers equipped with Peltier temperature controllers that maintained the measurement and incubation temperatures at 25 °C. Fluorescence experiments were carried out using semimicro (0.5 cm × 1.0 cm) or regular (1.0 cm × 1.0 cm) quartz cuvettes and in a HEPES/NaCl reaction buffer containing 0.1% PEG 8000 to prevent protein adsorption to the quartz surface. The excitation wavelength used for studying the fluorescence of PAI-$1_{121\text{-NBD}}$ was 480 nm, and the emission spectra were scanned from 500 to 650 nm using a bandwidth of 5 nm for both the excitation and emission beams. Emission spectra for PAI-$1_{121\text{-NBD}}$ (50−200 nM) were recorded prior to and after the addition of saturating concentrations of native vitronectin or recombinant SMB domain (0.2−1.0 μM) and a 5−10 min incubation period. The excitation wavelength for 4-FTrp PAI-1 was 300 nm, and the emission spectra were scanned from 320 to 450 nm using a bandwidth of 2.5 nm on the excitation beam and 5 nm on the emission beam. For these reactions, vitronectin (0.8 μM) was titrated with a 2−3-fold molar excess of 4-FTrp PAI-1 (1.6−2.4 μM), and changes in emission spectra were recorded after a 5−10 min incubation. Results are presented as the averaged spectra of three independent titrations. All individual emission spectra were collected as averages of 3−5 emission scans using 1.0 s integration over a 0.5 nm step resolution and corrected for background fluorescence and dilution effects, which were typically less than 5%.

Fluorescence Stopped-Flow Analysis of PAI-1: Vitronectin Binding Kinetics. Stopped-flow reactions of PAI-$1_{121\text{-NBD}}$ were measured on an Applied Photophysics SX.18MV stopped-flow reaction analyzer with a 25 °C thermostated syringe chamber. Excitation was at 480 nm, and a filter with a cutoff below 515 nm was used to monitor the fluorescence emission in the PAI-$1_{121\text{-NBD}}$ experiments. Unless otherwise stated, stopped-flow experiments were carried out under pseudo-first-order conditions with either native vitronectin or the recombinant SMB domain (0.05−1.0 μM) added in at least a 4-fold molar excess over PAI-$1_{121\text{-NBD}}$ (6.25−50 nM). Stopped-flow reaction traces representing the rapid increase in NBD fluorescence for reactions using PAI-$1_{121\text{-NBD}}$ were best fit to the single exponential function of eq 1 or the double exponential function of eq 2 to obtain the pseudo-first-order rate constants k_{obs-1} and k_{obs-2}:

$$F_t = F_0 + A_1(1 - e^{-k_{obs-1}t}) \quad (1)$$

$$F_t = F_0 + A_1(1 - e^{-k_{obs-1}t}) + A_2(1 - e^{-k_{obs-2}t}) \quad (2)$$

where F_t represents the fluorescence emission at time t (seconds), A_1 and A_2 are the amplitudes associated with k_{obs-1} and k_{obs-2}, respectively, and F_0 is the fluorescence at $t = 0$. The slope for the resulting linear dependencies of the k_{obs} values on the concentration of vitronectin gives the respective second-order association rate constants $k_{assoc-1}$ and $k_{assoc-2}$ depending on the selected model. The subsequent slow fluorescence change occurring after initial binding was associated with a single phase decrease in the NBD fluorescence, and therefore reaction traces were accordingly best fit by the expression of eq 3:

$$F_t = F_0 + Ae^{-k_{obs}t} \quad (3)$$

where F_t denotes the fluorescence emission at time t (seconds), A is the amplitude associated with the observed pseudo-first-order rate constant (k_{obs}), and F_0 is the fluorescence at time = 0.

Fluorescence Stopped-Flow Analysis of 4-FTrp PAI-1: Vitronectin Binding. Stopped-flow reactions of the 4-FTrp PAI-1 variant were measured on an Applied Photophysics SX.18MV stopped-flow reaction analyzer with a 25 °C thermostated syringe chamber. Excitation was at 300 nm, and a filter with a cutoff below 310 or 320 nm was chosen to exclude excitation light. Stopped-flow experiments were carried out both at a 1:1 ratio of 4-FTrp PAI-1 and native vitronectin and with 4-FTrp PAI-1 in excess. For reactions utilizing the 4-FTrp PAI-1 variant in excess, the observed slow conformational change was associated with a single-phase decrease in the intrinsic tryptophan fluorescence; therefore, reaction traces were accordingly best fit by the expression of eq 3.

Stopped-Flow Analysis of P9-NBD-Labeled PAI-1 Kinetics. Stopped-flow reactions of P9-NBD-labeled PAI-1 variants and their complexes with native vitronectin or the SMB domain were measured on an Applied Photophysics SX.18MV stopped-flow reaction analyzer with a thermostated syringe chamber. Excitation was at 480 nm, and a filter with a cutoff below 515 nm was used to monitor fluorescence emission. Stopped-flow experiments were carried out under pseudo-first-order conditions as has been previously described (*46*) with proteases in excess over the tested P9-NBD PAI-1

variants (6.25−25 nM). Reaction progress curves were typically monophasic, except as noted below, and best fit by the single exponential function of eq 1. As previously noted for tPA and uPA reactions occurring at high concentrations of protease, a slow linear increase in fluorescence persisted after the main exponential phase (*49*). In such cases, eq 1 was modified to include a finite linear function and assuming a finite end point. The amplitude of the linear fluorescence change was typically ≤10−15% of the total fluorescence increase and has been deemed to represent a slow isomerization of the P9-NBD fluorophore subsequent to the primary reaction step (*48, 49*). The k_{obs} values obtained for the major increase in fluorescence were subsequently analyzed assuming a two-step binding model (*46*) for which the dependence of k_{obs} on protease concentration is described by the function for a rectangular hyperbola:

$$k_{obs} = \frac{k_{lim}[P]_o}{K_M + [P]_o} \quad (4)$$

where $[P]_o$ is the protease concentration, k_{lim} represents the limiting first-order rate constant for the observed formation of a serpin−protease complex, and K_M is the concentration of protease at which the value of k_{obs} reaches one-half that of k_{lim} and is given by $(k_{lim} + k_{off})/k_{on}$, where k_{on} and k_{off} are the forward and reverse rate constants for formation of the noncovalent Michaelis complex, respectively (*46, 49*).

RESULTS

Stopped-Flow and Steady-State Fluorescence Measurements Using Probes on PAI-1 Indicate Differences in Binding of Full-Length Vitronectin and the SMB Domain. In order to follow the interaction of PAI-1 with vitronectin, we have engineered a PAI-1 variant with a single cysteine replacing a serine at a position that introduces a derivatizable free sulfhydryl moiety in the vicinity of the vitronectin binding domain. Based on a close proximity to the established region for vitronectin binding identified from biochemical and crystallization studies (*11*−*14*), the serine residue at position 121 (Figure 1) was chosen as the principal candidate for site-directed mutagenesis to create the S121C variant. Labeling with the environmentally sensitive NBD fluorophore produced the PAI-$1_{121\text{-NBD}}$ variant, with the probe located at a position intermediate between the binding site for the SMB domain of vitronectin and the second vitronectin-binding site that has been localized to the distal ends of helices D and E (*38*).

To follow the initial events defining the association of PAI-1 with vitronectin, we used pre-steady-state kinetic methods. Stopped-flow analyses of association reactions for native vitronectin with PAI-$1_{121\text{-NBD}}$ are characterized by a rapid enhancement in fluorescence (Figure 2A). Data acquisition at longer times (up to 200 s) revealed a slow decrease in NBD fluorescence following the rapid fluorescence enhancement phase (Figure 2A). The decrease in fluorescence typically reflected 25−30% of the initial fluorescence increase for reactions with native vitronectin. The association of PAI-$1_{121\text{-NBD}}$ with the isolated SMB domain also reflected a rapid rise in fluorescence (Figure 2A). However, the subsequent quench in fluorescence accounted for nearly 100% of the initial fluorescence enhancement.

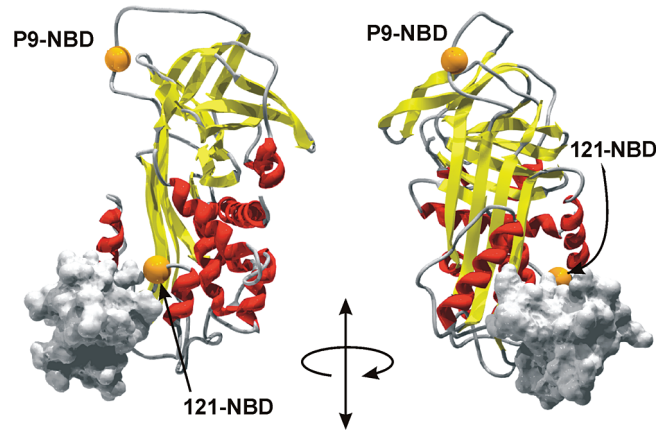

FIGURE 1: Localization of residues for fluorescent probe derivatization of the PAI-1 structure. The active (stressed) structure of PAI-1 (ribbon presentation) is depicted with the bound recombinant somatomedin B domain of vitronectin (surface representation). The β-sheet structures of PAI-1 are indicated in yellow, α-helices are indicated in red, and positions of fluorescent probe derivitization are indicated by orange spheres. The figure was generated in Swiss PDB Viewer (version 3.7 (*80*)), using the coordinates for active PAI-1 in complex with the recombinant somatomedin B domain (PDB id 1OC0 in ref *16*).

The emission spectra of the PAI-1−vitronectin and PAI-1−somatomedin B complexes were measured when the binding reaction had reached steady state (Figure 2B). The association of PAI-$1_{121\text{-NBD}}$ with native vitronectin results in a maximal enhancement of the fluorescence for the NBD probe of approximately 50% with a blue shift in the peak emission from 545 to 539 nm (Figure 2B). This observation indicates that the fluorophore becomes transferred into a more hydrophobic environment upon complex formation. Titration of 200 nM PAI-$1_{121\text{-NBD}}$ with increasing concentrations of native vitronectin demonstrated a stoichiometric and saturable change in NBD fluorescence, with a stoichiometry of 1:1 (Figure 2B, inset). A different result is seen upon association of PAI-$1_{121\text{-NBD}}$ with the SMB domain, with negligible fluorescent changes amounting to a slight 2% quench in total fluorescence (Figure 2B). This lack of a change in NBD fluorescence for equilibrium binding to the PAI-1 variant with the probe at position 121 is consistent with the data from the stopped-flow measurements (Figure 2A) that show an increase in fluorescence induced by the SMB domain within the first few milliseconds of binding, followed by a quench back to initial fluorescence values within ∼100 s.

Association of PAI-1 with Native Plasma Vitronectin Is a Two-Step Binding Process Followed by a Conformational Change. The rapid increase in fluorescence, followed by the slower decrease, observed when vitronectin or the SMB domain binds to PAI-$1_{121\text{-NBD}}$, is indicative of a sequence of events that characterize the association of the proteins. A first approach to the analysis was made as a fit to a two-step process, considering the most straightforward model to be a sequential reaction with two phases that correspond respectively to the rapid increase and slower decrease in fluorescence. Fits using this model for full-length vitronectin binding to PAI-$1_{121\text{-NBD}}$ were not satisfactory. One reason for the poor fits to the model is that our attempt to determine whether the rapid increase in fluorescence corresponded to a single event was not definitive when the fraction of data accounting for this early phase was less than 5% of the total reaction trajectory. The poor fits indicated that more than two rates

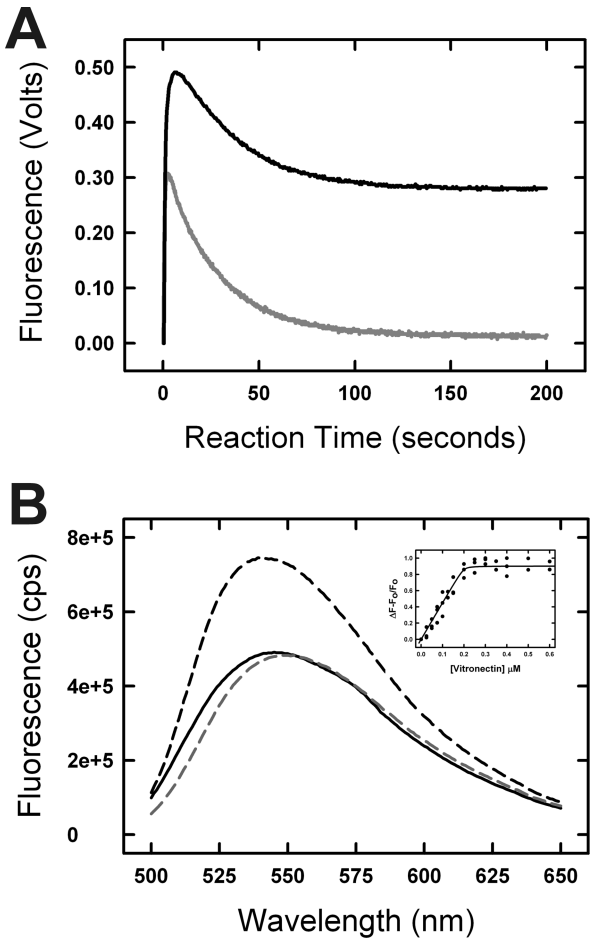

FIGURE 2: Fluorescent changes upon binding of vitronectin or its SMB domain to PAI-$1_{121\text{-NBD}}$. (A) Representative stopped-flow progress curves for reactions of 50 nM PAI-$1_{121\text{-NBD}}$ with 250 nM monomeric vitronectin (black trace) or recombinant SMB domain (gray trace). (B) Fluorescence emission spectra at steady state, following addition of monomeric vitronectin (200 nM) or recombinant SMB domain (200 nM) to PAI-$1_{121\text{-NBD}}$ (50 nM). Key: PAI-$1_{121\text{-NBD}}$ only (black trace); PAI-$1_{121\text{-NBD}}$ + monomeric vitronectin (black-dashed trace); PAI-$1_{121\text{-NBD}}$ + the SMB domain (gray-dashed trace). Inset: Equilibrium binding isotherm of 200 nM PAI-$1_{121\text{-NBD}}$ with monomeric vitronectin indicates a 1:1 stoichiometry of interaction. Results from experiments using an SMB domain isolated from plasma vitronectin by cyanogen bromide cleavage (native SMB domain) (*60*) demonstrated comparable results indistinguishable from those found with the SMB domain construct expressed in *P. pastoris* (data not shown).

were involved in the process and prompted a more detailed analysis of the rapid increase in fluorescence using stopped-flow methods to dissect the early events in the binding reaction.

Deconvolution of reaction traces for PAI-$1_{121\text{-NBD}}$ binding to native vitronectin (Figure 2A) revealed that the initial fast increase in PAI-$1_{121\text{-NBD}}$ fluorescence is biphasic, suggesting two events during the initial binding to vitronectin. To better characterize these binding events, reaction progress curves were measured on the fast time scale that focused on this initial increase in fluorescence for reactions of PAI-$1_{121\text{-NBD}}$ with a 10-fold molar excess of native vitronectin or the SMB domain in order to maintain pseudo-first-order conditions (Figure 3). The dual-phase character of the reaction progress curves with monomeric plasma vitronectin, but not with the SMB domain, is best appreciated by comparing the deviations in residual values that arise when evaluating fits of

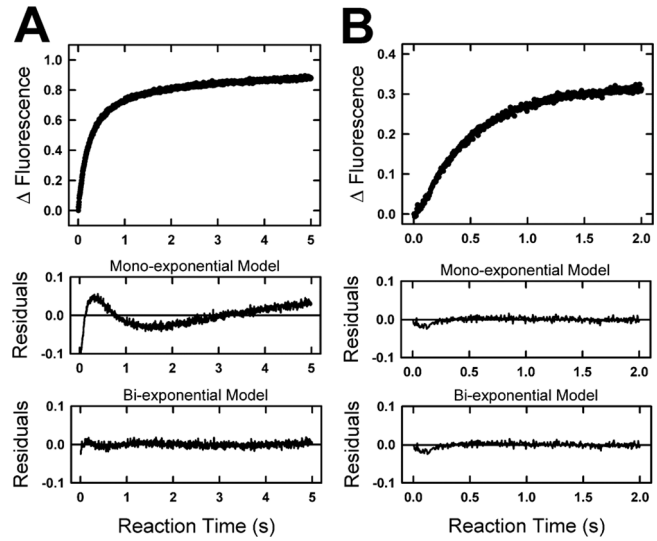

FIGURE 3: Analyses of fluorescence stopped-flow progress curves demonstrate multiphase association kinetics with native vitronectin but not the SMB domain. Shown are stopped-flow progress curves of 50 nM PAI-$1_{121\text{-NBD}}$ with 250 nM monomeric vitronectin (panel A) or 250 nM recombinant SMB domain (panel B). Residual plots for mono- and biexponential models (eqs 1 and 2 in Experimental Procedures, respectively) are illustrated below the individual progress curves in panels A and B.

monoexponential versus biexponential models (Figure 3, lower panels). Analyses of the residual arrays from the two regression models by the *F*-test statistic to determine the best fit model yielded *p*-values of $p < 0.001$ (native vitronectin) and $p = 1.000$ (SMB domain), supporting the idea that the reaction with native vitronectin is best modeled by a biexponential regression analysis, while data with the SMB domain are fit adequately to a single kinetic phase. The different result comparing the SMB domain versus full-length vitronectin binding to PAI-$1_{121\text{-NBD}}$ underscored the importance of pursuing the detailed analysis using pre-steady-state kinetics to clarify the steps in the reaction that were not easily modeled by a two-step, sequential binding model. If the second, slower phase of the binding reaction were somehow skewing the analysis during the rapid phase with an increase in fluorescence, we would expect the same artifacts to arise with the SMB domain, which has the same two reaction phases. However, there is a clear difference between the SMB domain, with one binding site for PAI-1, and full-length vitronectin, with two binding sites (*37, 38*), that result in one or two exponentials, respectively, in the early phase of the binding reaction.

Reaction progress curves for experiments with native vitronectin were thus analyzed as a biexponential process according to eq 2, yielding the two observed rate constants, k_{obs-1} and k_{obs-2}. Progress curves for reactions of the SMB domain with PAI-$1_{121\text{-NBD}}$ were fit using the single exponential in eq 1, yielding only k_{obs-1}. The relative fluorescence amplitudes observed for the two reaction rates with native vitronectin each accounted for approximately one-half of the total fluorescence increase. An exception was observed at the highest concentrations of native vitronectin (>0.5 μM), where the fluorescence signal associated with k_{obs-2} (the slower rate) typically predominated. For reactions of PAI-$1_{121\text{-NBD}}$ with the SMB domain, the maximal fluorescence enhancement was routinely 40−50% of that observed for native vitronectin progress curves. This observation is

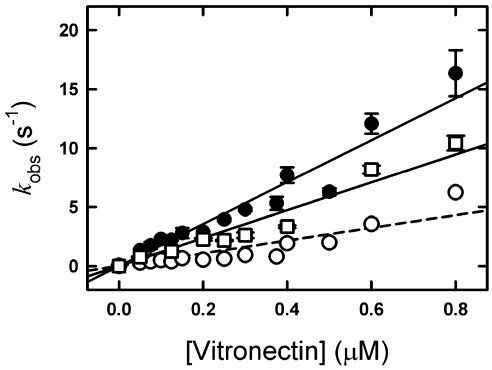

FIGURE 4: Stopped-flow kinetics to determine association rates for PAI-1 interaction with vitronectin or the SMB domain. Reactions of PAI-$1_{121\text{-NBD}}$ with vitronectin were monitored in a stopped-flow experiment to obtain pseudo-first-order k_{obs-1} and k_{obs-2} values for the mono- and biphasic reactions of vitronectin variants, which were plotted against the vitronectin concentration as described in Experimental Procedures. "Fast-phase" k_{obs-1} values (solid) and "slow-phase" k_{obs-2} values (open) are shown for native monomeric vitronectin (solid and open circles) and recombinant SMB domain (open squares). Solid (fast-phase) and dashed (slow-phase) lines represent linear regression fits of the data assuming a zero intercept.

consistent with binding of the SMB domain accounting for half of the total probe perturbation, while additional molecular interactions of full-length vitronectin accounts for the ancillary fluorescence changes (compare curves in Figures 2 and 3).

The dependencies of the observed association rates on increasing concentrations of native vitronectin or the SMB domain are shown in Figure 4. In all cases, the evaluated k_{obs-1} values (and k_{obs-2} values measured only for native vitronectin reactions) were nonlimiting and linear over the experimentally accessible concentration range (0.05−1.0 μM). This direct concentration dependence indicates that the experiments monitor two noncovalent binding events between PAI-1 and native vitronectin during the fast reaction phase, while only single association events are observed for binding to the SMB domain.

Evaluation of the linear dependencies for k_{obs-1} and k_{obs-2} on the vitronectin concentration allows a determination of the corresponding values for the association kinetics of these two binding interactions with second-order association rate constants equal to $k_{assoc-1}$ of $(1.88 \pm 0.10) \times 10^7$ M^{-1} s^{-1} and $k_{assoc-2}$ of $(7.13 \pm 0.35) \times 10^6$ M^{-1} s^{-1}. The $k_{assoc-1}$ values for native vitronectin and the SMB domain ($(1.37 \pm 0.06) \times 10^7$ M^{-1} s^{-1}) are comparable, suggesting a fast, high-affinity interaction with the SMB domain. In addition, the biphasic reaction profile with native vitronectin indicates that there is a second interaction event that occurs at a ∼2−3-fold slower rate and/or is of a lower affinity.

Whereas the initial rapid increase(s) in NBD fluorescence for each tested vitronectin variant followed a linear concentration dependence, the slower subsequent decrease in NBD fluorescence that occurs on longer time scales (k_{obs-3}) represents a phase of the reaction that is independent of vitronectin concentration. These monophasic fluorescence quenches acquired at 25 °C were analyzed by eq 3, yielding rate values in the range of 0.03−0.04 s^{-1} for reaction traces with full-length vitronectin or the SMB domain. The saturable nature of this slow phase provides evidence that the NBD probe on PAI-1 monitors a structural change that occurs after the initial fast binding reaction. The fact that the rate of the conformational change is saturated at the lowest tested vitronectin concentration (50 nM) is consistent with the observed high affinity for PAI-1 binding to native vitronectin, with K_d's for the SMB domain and the second site equal to 0.1−1 nM (*57*) and ∼25−50 nM (*37, 38*), respectively.

Structural Changes Occur in Vitronectin after Binding to PAI-1. The fluorescence stopped-flow results presented in Figure 2A indicate a change in conformation that occurs after binding of a single PAI-1 molecule to the SMB domain of vitronectin but do not distinguish whether the structural change occurs only in PAI-1 or both proteins in the complex. Indeed, it is possible that conformational changes within the SMB domain of vitronectin could be a primary contributor to changes in the fluorescence of the probe on PAI-1 because of the intimate binding interface at which the NBD probe is found. We therefore sought an approach that would solely monitor conformational perturbations in vitronectin when bound to PAI-1, testing the long-standing hypothesis that PAI-1 binding elicits an alteration in vitronectin. In order to exclusively monitor vitronectin using its intrinsic tryptophan fluorescence, we have exploited a novel variant of PAI-1 that was engineered to be "fluorescently silent" (*52*). This was accomplished through the biosynthetic incorporation of a 4-fluorotryptophan analogue of tryptophan into PAI-1 during recombinant protein expression, thus creating a variant that functions essentially like the wild-type protein but which effectively has no observable fluorescence when excited at 300 nm (*52*). Thus, any intrinsic fluorescence measured arises from the eight tryptophans in vitronectin, which are located at positions 181, 201, 261, 294, 303, 382, 405, and 450. Most of these tryptophans are localized within the C-terminal half of vitronectin, and none of these are found within the SMB domain. As shown in Figure 5A, the addition of a 2-fold molar excess of 4-FTrp PAI-1 to monomeric vitronectin (0.8 μM) results in a quenching of the intrinsic tryptophan fluorescence of native vitronectin, with a maximal saturating quench of 22.8%. Further addition of 4-FTrp PAI-1 did not result in any additional quenching of the vitronectin fluorescence. The fluorescence quench occurred on a time scale that was considerably faster than that previously reported for PAI-1 induced oligomerization of vitronectin (*35*). Furthermore, incubation of the 4-FTrp PAI-1−vitronectin complexes at 37 °C after the initial quench did not produce any additional change in intrinsic tryptophan fluorescence over a time period of up to 60 min (data not shown), conditions under which higher order oligomers are known to accumulate (*35*). The absence of any detectable changes in tryptophan fluorescence, and consequently, transitions in the vitronectin structure when monitored over this longer time frame, is consistent with the initial binding of PAI-1 to native vitronectin triggering the observed conformational change in vitronectin.

In order to further elucidate the nature and rate of the conformational change in native vitronectin induced by the binding of 4-FTrp PAI-1, reactions were followed by stopped-flow fluorometry using a 1:1 stoichiometry of 4-FTrp PAI-1 and native vitronectin (Figure 5B). Inspection of the time courses from stopped-flow experiments revealed that the observed rate of intrinsic tryptophan fluorescence quenching represents a monophasic, concerted transition within the vitronectin structure as monitored by intrinsic tryptophan

Table 1: Individual Rate Constants for Protease Inhibition by PAI-1 Mutants in the Presence of Native Vitronectin or the SMB Domain[a]

	tPA			uPA		
	k_{lim} (s^{-1})	K_M (μM)	k_{lim}/K_M (μM^{-1} s^{-1})	k_{lim} (s^{-1})	K_M (μM)	k_{lim}/K_M (μM^{-1} s^{-1})
wild type	2.26 ± 0.01	0.06 ± 0.01	37.67	14.49 ± 0.53	1.19 ± 0.13	12.18
wild type + nVN	2.25 ± 0.03	0.12 ± 0.01	18.75	5.45 ± 0.13	0.86 ± 0.05	6.34
wild type + rSMB	2.27 ± 0.02	0.07 ± 0.01	32.43	6.58 ± 0.12	0.48 ± 0.03	13.71
E352A/E353A	10.09 ± 0.42	2.30 ± 0.20	4.39	18.87 ± 1.01	4.22 ± 0.40	4.48
E352A/E353A + nVN	3.31 ± 0.16	0.90 ± 0.11	3.69	4.33 ± 0.15	2.43 ± 0.18	1.78
E352A/E353A + rSMB	6.09 ± 0.26	1.14 ± 0.13	5.33	6.24 ± 0.20	1.53 ± 0.12	4.07
R117E/R120E	2.18 ± 0.02	0.06 ± 0.01	38.93	15.68 ± 0.81	1.85 ± 0.19	8.49
R117E/R120E + nVN	2.29 ± 0.02	0.16 ± 0.01	14.83	9.35 ± 0.44	1.73 ± 0.16	5.51
R117E/R120E + rSMB	2.61 ± 0.04	0.11 ± 0.01	23.13	10.53 ± 0.62	0.75 ± 0.12	14.10
K325A	1.56 ± 0.01	0.06 ± 0.01	26.00	15.54 ± 0.46	1.43 ± 0.09	10.90
K325A + nVN	2.19 ± 0.06	0.13 ± 0.02	16.47	7.59 ± 0.42	1.19 ± 0.17	6.34
K325A + rSMB	2.37 ± 0.02	0.10 ± 0.01	23.70	9.78 ± 0.19	0.72 ± 0.05	13.70
Stab	0.20 ± 0.01	0.06 ± 0.01	3.20	5.66 ± 0.15	0.46 ± 0.04	12.30
Stab + nVN	0.60 ± 0.01	0.10 ± 0.01	6.10	6.55 ± 0.22	1.28 ± 0.09	5.10
Stab + rSMB	0.25 ± 0.01	0.08 ± 0.01	3.13	6.72 ± 0.16	0.69 ± 0.45	9.68
Stab-R117E/R120E	0.37 ± 0.01	0.13 ± 0.01	2.85	5.28 ± 0.10	0.61 ± 0.03	8.69
Stab-R117E/R120E + nVN	0.48 ± 0.01	0.14 ± 0.02	3.42	6.86 ± 0.23	1.37 ± 0.10	5.03
Stab-R117E/R120E + rSMB	0.35 ± 0.01	0.14 ± 0.01	2.50	9.08 ± 0.44	1.22 ± 0.14	7.43

[a] Rapid kinetic experiments were measured in 0.03 M HEPES/0.135 M NaCl/1 mM EDTA at pH 7.4 and 25 °C. Data are reported as the best fit to the stopped-flow data ± SE of the fit. The second-order rate constant for PAI-1 inhibition of proteases was calculated from the fitted stopped-flow data as k_{lim}/K_M.

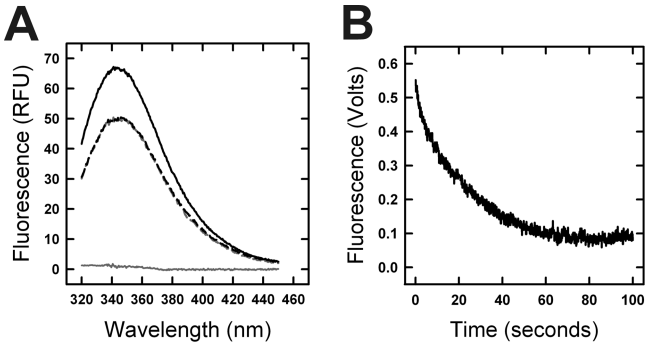

FIGURE 5: Intrinsic tryptophan fluorescence changes indicate a transition in the structure of plasma vitronectin upon interaction with PAI-1. (A) Addition of 4-FTrp PAI-1 to 0.8 μM monomeric vitronectin: vitronectin only (black trace); vitronectin + 1.6 μM 4-FTrp PAI-1 (2:1 ratio) (black-dashed trace); vitronectin + 2.4 μM 4-FTrp PAI-1 (3:1 ratio) (gray-dashed trace); control fluorescence of 0.8 μM 4-FTrp PAI-1 (gray trace). (B) Representative stopped-flow progress curve for the reaction of 1.2 μM 4-FTrp PAI-1 with 0.1 μM full-length vitronectin was recorded in a stopped-flow reaction analyzer over a 100 s time interval as described in Experimental Procedures.

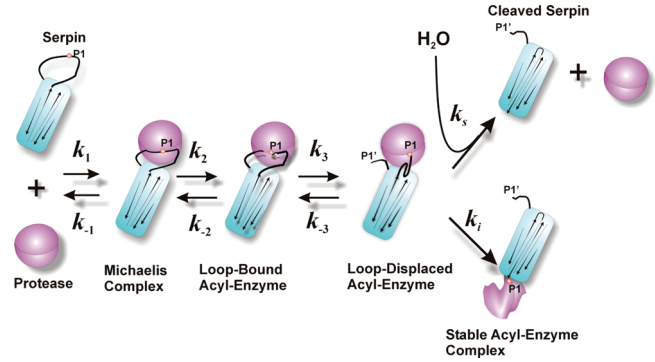

FIGURE 6: Schematic representation of the serpin inhibition reaction with a protease. The reaction is initiated by the formation of a noncovalent Michaelis complex (k_1/k_{-1}) followed by proteolytic cleavage of the P1−P1′ peptide bond to give a reversible loop-bound acyl-enzyme intermediate (k_2/k_{-2}). The limiting rate step, which is insertion of the first hinge residue(s) into the breach region (k_3/k_{-3}) (*50*), gives a loop-displaced intermediate with a release of the distal P′ fragment from the substrate pocket of the protease. This step permits complete loop insertion ($k_i + k_s$) as an inhibited acyl-enzyme complex or hydrolyzed serpin and free protease.

fluorescence. The fluorescence quench occurs on a similar time scale as that of the slow conformational change reported by the NBD probe on PAI-$1_{121\text{-NBD}}$. Pseudo-first-order reactions with varying 4-FTrp PAI-1 concentrations (0.4−3.0 μM) in excess over native vitronectin (0.1 μM) were measured, yielding monophasic quenches in tryptophan fluorescence with k_{obs} values between 0.02 and 0.05 s^{-1} (data not shown). The fact that the observed reaction rates only marginally increase over a large concentration range argues that the PAI-1 induced changes in intrinsic tryptophan fluorescence report a structural transition in plasma vitronectin and that the reaction rate is close to saturation at the lowest tested 4-FTrp concentrations.

Differential Rates of Reaction of Target Proteases with PAI-1 in Complex with Vitronectin or the SMB Domain. Also of interest was whether the binding of vitronectin or the SMB domain affects the characteristic mechanism of inhibition of proteases by PAI-1. To evaluate these effects, we used a well-described fluorescence model for monitoring the transient reaction kinetics of PAI-1 inhibition of target proteases (*48*), measuring the effects of native vitronectin and the SMB domain on the rate of reactive center loop (RCL) insertion. For this model system, the PAI-1 molecule was labeled at the P9 residue with NBD in order to follow RCL insertion by stopped-flow fluorometry (Figure 1). Our prior studies (*40, 43, 46*) and those of others (*49, 58*) have established multiple steps in the serpin reaction pathway, which are illustrated by Figure 6, showing an expanded model for protease inhibition by serpins in which the overall limiting rate (k_{lim}) includes several mechanistic steps. These include reversible acylation of the acyl-enzyme intermediate (k_2 and k_{-2}), release of the P′-side of the RCL from the protease active site cleft (k_3 and k_{-3}), and loop insertion (k_i and k_s) (*43, 46, 49*). In the case of PAI-1 where strong exosite interactions persist with its target proteases, it has been shown that the primary rate-limiting step is release of the P′-side of the RCL from the protease active site (k_3) (*43, 46*). Whereas both native vitronectin and the SMB domain had

negligible effects on the limiting rate of RCL insertion (k_{lim}) for reactions of wild-type PAI-1 with tPA, a significant reduction in k_{lim} was noted when uPA was used as the target protease (Table 1). Such an observation indicates that the binding of the SMB domain of vitronectin affects the PAI-1 structure and effectively increases the thermodynamic energy barrier for loop insertion when uPA is the target protease.

In order to more fully understand these tPA vs uPA differences and characterize the effects of native vitronectin or the SMB domain on the mechanism of PAI-1 inhibition, we expanded our approach by using a panel of selected PAI-1 variants that can distinguish various points along the reaction pathway presented in Figure 6. Previous work has demonstrated that reactions of PAI-$1_{P9\text{-}NBD}$ with tPA or uPA yield a k_{lim} that is dominated by the rate of release of the P′-side of the cleaved RCL from the substrate cleft of the protease with a concomitant breaking of exosite−exosite interactions between the acidic P4′−P5′ glutamate residues of PAI-1 and basic residues on the 37-loop of the proteases (*43, 46*). The exosite interactions are stronger for PAI-1 with tPA compared to uPA, which is one reason that the overall limiting rate of RCL insertion is higher for uPA. This step that occurs upon breaking of these exosite interactions is represented by the transition of a loop-bound acyl-enzyme intermediate to that of a loop-displaced acyl-enzyme intermediate (k_3/k_{-3}) in the scheme illustrated by Figure 6, with residues in the vicinity of P12 to P14 inserted into the top of the central β-sheet. Introduction of alanine substitutions at the P4′ and P5′ residues (E352A/E353A) yielded the expected increase in k_{lim}, due to disruption of the exosite interactions (*43, 46*). However, the binding of native vitronectin or the SMB domain to this exosite mutant of PAI-1 resulted in a significant reduction in k_{lim} for both tPA and uPA reactions (Table 1 and Figure 7A). The extent of reduction in k_{lim} was greater when native vitronectin was used as compared to the SMB domain for both tPA and uPA reactions (Table 1). This result indicates that full-length native vitronectin has additional stabilizing interactions that are mediated by regions outside of the SMB domain.

Residue K325 was previously postulated to play a role in RCL insertion in the serpin mechanism by anchoring β-strand 5A through side-chain hydrogen bonding to the loop connecting α-helix F to β-strand 3A (*59*). Replacement of K325 with alanine disrupts this interaction that stabilizes the central β-sheet, allowing for more facile insertion of the RCL during the course of the serpin mechanism. For uPA reactions, the K325A mutation had no effect on the basal rate of protease inhibition in the absence of vitronectin. However, the k_{lim} for K325A PAI-1 reaction with uPA was decreased in the presence of native vitronectin or the SMB domain. Nevertheless, these reduced rates for RCL insertion upon reaction with uPA were less pronounced than the corresponding effects on k_{lim} with wild-type PAI-1 (Table 1). In contrast, for reactions of the K325A PAI-1 with tPA there was a decrease in the basal k_{lim} value and a slight increase in the rate of reaction in the presence of both vitronectin variants.

By far the most prominent effect on k_{lim} was observed with the latency resistant, stable variant of PAI-1 containing the four mutations described by Berkenpas et al. (*45*). Reaction of the stable variant of PAI-1 with tPA in the absence of vitronectin is characterized by an order of magnitude reduction in k_{lim} (0.2 vs 2.3 s^{-1}), whereas the reaction is only reduced 3-fold when uPA is the target protease. The basis for the effects on k_{lim} for these PAI-1

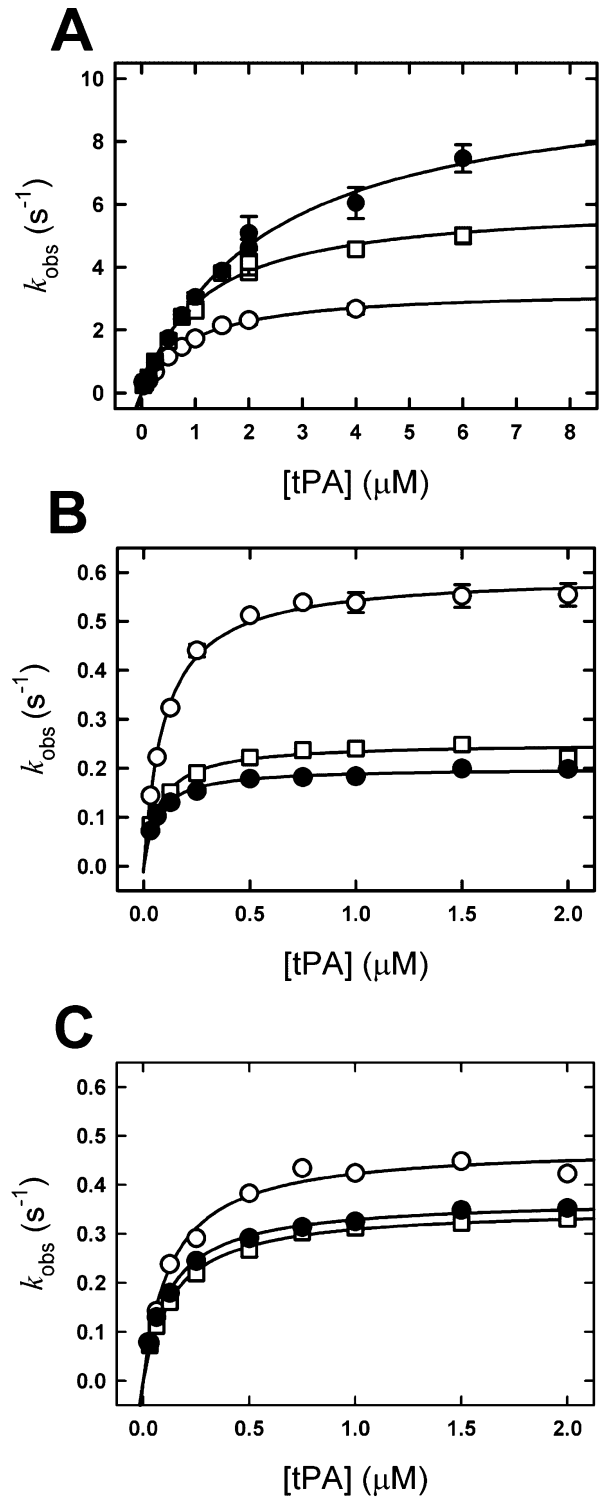

FIGURE 7: Differential effect on the limiting rate (k_{lim}) for protease inhibition by PAI-1 in the presence of full-length vitronectin or the SMB domain. Stopped-flow analyses for select PAI-$1_{P9\text{-}NBD}$ variants (6.25−50 nM) in the absence of vitronectin (●), or in complex with 50 nM vitronectin (○) or recombinant SMB domain (□). Reactions with increasing concentrations of tPA (0.05−6 μM) were carried out in a stopped-flow reaction analyzer as described in Experimental Procedures. Averaged k_{obs} values from 6−10 experiments were plotted and fit to eq 4 in Experimental Procedures (solid lines) to obtain the k_{lim} values reported in Table 1. E352A/E353A PAI-$1_{P9\text{-}NBD}$ (panel A); Stab PAI-$1_{P9\text{-}NBD}$ (panel B); Stab - R117E/R120E PAI-$1_{P9\text{-}NBD}$ (panel C).

variants is likely similar to that described previously for a stabilizing mutation in the conserved breach region of PAI-1 (*46*). In striking contrast to our observations with other PAI-1 variants, full-length native vitronectin but not the SMB domain accelerated the reaction rate of the stable PAI-1 variant with tPA by a factor of 3 (Table 1 and Figure 7B). There was no apparent effect of either vitronectin variant on reactions with uPA. Such discrepancies regarding the effects of full-length vitronectin and the SMB domain on rates of RCL insertion for the stable PAI-1 variant are consistent with more extensive interactions with native vitronectin outside of the SMB domain. For this "stable" PAI-1 variant these interactions permit an accelerated reaction; nevertheless, the data also indicate that discrete structural differences likely exist between the stable mutant and wild-type PAI-1. This observation is consistent with a recent report by Li et al. (*60*), who postulate that the stable variant of PAI-1 has distinct structural differences compared to native wild-type PAI-1 in the proximity of the breach.

Our recent studies (*37, 38*) provide evidence for an extended binding interaction between PAI-1 and a recombinant variant of vitronectin lacking the SMB domain (rΔsBVN), which is primarily dependent on a patch of basic residues along α-helices D and E. A double mutation of PAI-1 constructed within this extended binding site and having charge reversals corresponding to the R117E and R120E substitutions was shown to strongly reduce binding to rΔsBVN (*38*). We have also used this charge reversal mutant to test for differential effects on RCL insertion upon binding to the SMB domain or to full-length vitronectin (Table 1). For reactions with uPA, the R117E/R120E mutation demonstrated less of a reduction in the k_{lim} compared to wild-type PAI-1. Also, the effects of full-length vitronectin were comparable to those observed with the SMB domain alone, consistent with a mutation that disrupts interactions at the second binding site (*37, 38*). Consistently, incorporation of the R117E-R120E charge reversal mutations along with those in the 14-1B "stable" form of PAI-1 neutralized the accelerated k_{lim} observed for the reactions of stable PAI-1 with tPA in the presence of native vitronectin; however, only small effects were observed on reactions in the absence of native vitronectin or the SMB domain (Table 1 and Figure 7C).[2] The generation and analysis of multiple mutants and their inhibition of both proteases were necessary to discern the effects of disruption of one of the binding sites for vitronectin on the RCL insertion and the overall serpin inhibition mechanism. The separate effects for primary site and secondary site binding that are suggested, comparing the R117E-R120E double mutant with wild-type PAI-1, are much more obvious in the case where kinetics are measured using the stable mutant of PAI-1 ± the added mutations. In summary, these functional data with a variety of PAI-1 mutants support the view that native vitronectin has interactions with PAI-1 that extend beyond those of the SMB domain. As seen from the data, these interactions can have noteworthy effects on the mechanism of PAI-1 inhibition.

[2] It is possible that the double mutation has an effect on the conformation of PAI-1 in this region, as the basal k_{lim} value for the stable variant containing the R117E/R120E mutation was also slightly accelerated, and uPA reactions showed a marginally increased k_{lim} in the presence of native vitronectin or the SMB domain.

DISCUSSION

Presently, the biological role for vitronectin is debated, as its known biochemical functions are multifaceted, involving numerous interactions with a variety of biomolecules from several physiological pathways, including coagulation, fibrinolysis, inflammation, pericellular proteolysis, and cell adhesion (*10, 22, 23, 61*−*64*). PAI-1 also has a role in these processes, and these two partner proteins are often found to be colocalized in the extracellular compartment (*26*−*28, 65*). The present study was undertaken to shed further light on the molecular interactions that transpire between PAI-1 and vitronectin, using pre-steady-state kinetics to focus on the early stages of the interaction. Our findings establish that a rapid, two-step association occurs between PAI-1 and full-length monomeric vitronectin that confers conformational changes to both molecules. Furthermore, a variety of approaches indicate that the binding of PAI-1 to full-length vitronectin involves a more extensive interaction surface that covers regions outside of the well-characterized binding site for the SMB domain on PAI-1.

Two Sites of Interaction between PAI-1 and Vitronectin. In most work to date, only a single, well-defined binding site on PAI-1 for vitronectin has been characterized using several biochemical (*11, 12, 14, 57*) and structural methods (*13, 56, 66*). In these studies, vitronectin was shown to interact with a region of PAI-1 that bridges a hydrophobic pocket spanning from α-helices D and E to α-helix F and covering strands s1A and s2A of β-sheet A (*1*). Although binding is thought to mainly involve hydrophobic interactions, a strong ionic interaction was found with Arg^{103} residing on the α-helix E-s2A turn of PAI-1 (*11*−*14*). The complementary PAI-1-binding region has been identified as a high-affinity (K_d ~0.5−10 nM) site within the amino-terminal SMB domain (residues 24−30) (*13, 56, 67*).

For a long time, other somewhat controversial reports have suggested the presence of a putative second lower affinity domain for PAI-1 elsewhere in the vitronectin molecule (*32, 33, 68*). From previous studies by some of us, the conclusion was drawn that two molecules of PAI-1 can bind to vitronectin under some circumstances (*8, 36*), causing us to evaluate the possibility of a second binding site in earnest. Work with a deletion mutant lacking the SMB domain, referred to as rΔsBVN, allowed for screening a variety of PAI-1 mutants in order to show that interactions with vitronectin extend to distal regions of helices D and E on PAI-1 (*37, 38*). Our evaluation in this study of the rapid kinetics of interaction was prompted by the demonstration of additional binding sites on PAI-1 and vitronectin.

A better understanding of the early events that characterize the association of PAI-1 and vitronectin was afforded by evaluating the relative rates of these initial binding steps and identifying potential conformational changes using a sensitive fluorescent probe placed in close proximity to the boundary of the SMB domain binding pocket. This approach shows that the association of PAI-1 with monomeric vitronectin consists of distinct phases of binding. A two-step, noncovalent association and a subsequent slow conformational change in the tertiary structure of vitronectin and/or PAI-1 are observed (Figures 2, 3, and 5). The most reasonable interpretation for the biphasic association observed with full-length native vitronectin, which is absent in reactions using

the isolated SMB domain (Figure 3), is the engagement of the more extensive interaction surface that encompasses residues outside the SMB domain.

Given that equilibrium titrations conducted under similar conditions as the stopped-flow binding analyses describe a 1:1 stoichiometry with native monomeric vitronectin (Figure 2A, inset), along with the fact that two reaction phases are not observed in reaction transients using the isolated SMB domain, the data support a model in which a single vitronectin molecule binds to PAI-1 at two interfaces. The approximate 3-fold difference in k_{assoc} values for the two native vitronectin binding events is consistent with this model and the notion that the secondary binding site lies outside the SMB domain. These findings are also consistent with the enhanced fluorescence reported by the binding of PAI-$1_{121\text{-NBD}}$ to full-length native vitronectin relative to that of binding to the SMB domain (Figures 2B and 3). Our previous analytical ultracentrifugation work pointed to the role of two binding sites that can accommodate two separate molecules of PAI-1 on a single vitronectin molecule (*36*). However, the conditions used in our present kinetic measurements do not favor such higher order assembly. The stopped-flow experiments were conducted under pseudo-first-order conditions with vitronectin in excess. Such conditions are not conducive to the binding of >1 molecule of PAI-1 to vitronectin. Instead, it appears that, under these conditions, a single molecule of vitronectin can interact with a single molecule of PAI-1 via two binding events at two sites. However, a strict order of binding is not dictated by the data. If, in fact, binding to the SMB domain were obligatory before binding to the second site via an intramolecular process, we would expect the rate constant for binding to the second site to be extremely rapid, not slower than the first association rate. Therefore, although a preferred order of binding will be dictated by differences in dissociation constants, the bimolecular nature of the two binding events indicates that a strict, sequential binding process is not observed. Whether the second binding site characterized by this and our other recent studies (*37, 38*) has a direct relation to the higher order structures observed by analytical ultracentrifugation remains to be established.

Conformational Changes Occur in Both upon Binding of Vitronectin to PAI-1. The change in the fluorescence of the NBD probe on the engineered Cys_{121} in PAI-1 on a slower time scale is compatible with a conformational change that occurs subsequent to the dual binding events. Our working hypothesis is that a concomitant change in the structure of vitronectin occurs upon binding to PAI-1. In support of this idea, vitronectin has been reported to undergo an irreversible conformational change into an "altered" state that is readily incorporated into the ECM and is prevalent in damaged tissues and in pathological disease states (*28, 35, 65*). The modified spectroscopic properties of the 4-FTrp PAI-1 variant have effectively silenced any intrinsic fluorescence of PAI-1 and for the first time allowed a direct visualization of the structural change that occurs in vitronectin upon complex formation with PAI-1 (Figure 5). The slower nature of this conformational transition compared to the rapid formation of the PAI-1−vitronectin encounter complex supports our prediction that the binding of PAI-1 to full-length monomeric vitronectin induces a conformational change subsequent to binding.

Extensive Interactions between PAI-1 and Vitronectin, Including Interfaces Outside of the SMB Domain, Affect the Mechanism by Which the Serpin Inhibits Target Proteases. The primary function of serpins such as PAI-1 is their inhibition of target proteases via formation of a 1:1 stable, inactive, acyl-enzyme complex via the mechanism illustrated in Figure 6. Accessory proteins or cofactors may bind to serpins and influence the rates of the individual steps along the reaction sequence, ultimately affecting the limiting rate and products formed in the pathway. The role of vitronectin in stabilizing PAI-1 (*69, 70*), in affecting the orientation of its RCL (*12, 71, 72*), and in influencing its protease inhibition repertoire (*73*) have been studied. We exploited the availability of full-length vitronectin to compare with the isolated SMB domain, along with several mutant forms of PAI-1, to assess effects of vitronectin on the mechanism of protease inhibition by PAI-1. Our working hypothesis is that more extensive interactions occur with full-length vitronectin versus the isolated SMB domain and that these can affect the serpin mechanism in different ways. To evaluate the protease inhibitory mechanism for PAI-1, we utilized an NBD label introduced strategically into position P9 of the RCL, which has been shown to provide a sensitive reporter for determining the limiting rate of RCL insertion (k_{lim}) into the central β-sheet of PAI-1 in the course of the inhibitory pathway. According to the mechanism depicted in Figure 6, k_{lim} is a compound rate constant consisting of several mechanistic steps that are described by the simplified expression $k_2k_3^*/(k_2 + k_{-2} + k_3^*)$, where k_3^* equals $k_3(k_i + k_s)/(k_{-3} + k_i + k_s)$ (*46*).

Results with tPA and uPA do not mirror each other, with vitronectin and the SMB having differential effects that vary according to which protease is tested in the assay. Protease-specific effects with PAI-1 have been observed previously in mutational analysis, due to a large extent to the more prominent contribution of exosite interactions in the serpin reaction scheme for tPA versus uPA. Furthermore, the magnitude and direction of the effects of full-length vitronectin and the SMB domain on limiting rates of loop insertion vary among PAI-1 variants tested. Most notably, in several cases, full-length vitronectin affects the limiting rate to a greater extent than does the SMB domain alone. Moreover, we have now identified a charge reversal (R117E-R120E) mutant form of PAI-1 that is defective at binding vitronectin over the full extent of the binding surface, disrupting interactions that occur in addition to those with the SMB domain from vitronectin (*38*). This mutant form of PAI-1 exhibits less pronounced differences in effects on loop insertion comparing full-length vitronectin and the SMB domain, consistent with the disruption of important contacts between the two proteins.

Recently, Komissarov and colleagues have taken a similar approach, utilizing P9-labeled PAI-1 and the SMB domain to evaluate effects of vitronectin and monoclonal antibodies on the mechanism of protease inhibition by PAI-1 (*74*). As in our work, these authors observed decreases in the limiting rate of RCL insertion for several proteases in the presence of the SMB domain and also noted differential effects compared to using full-length vitronectin (*75*). They have suggested that a decreased rate of RCL insertion with the SMB domain is a result from stabilization of another intermediate along the serpin reaction pathway in addition

to those depicted in the canonical scheme shown in Figure 6. This conclusion is drawn in part from results of kinetic measurements on RCL insertion with the SMB domain plus a monoclonal antibody, both of which bind in the vicinity of the α-helix F. According to their interpretation, the role of the SMB domain is to impede RCL insertion via this "helix F" intermediate that is heretofore uncharacterized. Instead, our data support a simpler model in which the stabilization of loop insertion by vitronectin occurs at a known point along the pathway, i.e., at the stage in which the proximal loop first inserts into the breach region of the serpin (k_3/k_{-3} in Figure 6) (*46*). This effect was revealed most effectively by using the E352A-E353A mutant that disrupts the exosite interactions that are rate-limiting for formation of the loop-displaced intermediate with partial insertion of the P-side residues into the central β-sheet. Relief of these interactions so that loop insertion can proceed relatively unimpeded allowed for the direct observation of vitronectin effects in the serpin pathway. Since insertion of the RCL into the central β-sheet is known to weaken interactions of PAI-1 with vitronectin (*76*), a plausible mechanism for stabilization of the loop-bound intermediate is that proceeding along the reaction pathway to the loop-displaced intermediate, in which the N-terminal portion of the RCL becomes partially inserted into the sheet A at the center of the serpin, would be disfavored because it would result in disrupted binding of vitronectin. Indeed, the binding of vitronectin at the base of the central β-sheet is thought to prevent the mobility of strands 3A and 5A, which is required for the RCL to insert. This interpretation is consistent with several new lines of evidence presented here including the use of the "exosite" mutant of PAI-1 to highlight differences in the kinetics with vitronectin and the SMB domain, the demonstrated concomitant conformational changes in PAI-1 and vitronectin, and evidence for more extensive binding interactions between PAI-1 and full-length vitronectin. Recent NMR and deuterium exchange studies have also supported our interpretation that the binding of the SMB domain alone confers a conformational change in the PAI-1 structure.[3] Thus, we favor a model in which interactions can form between full-length vitronectin that extend beyond those contributed by the SMB domain and act to stabilize this intermediate and consequently affect the mechanism by which PAI-1 inactivates target proteases.

ACKNOWLEDGMENT

Dr. Joseph D. Shore, formerly head of the Division of Biochemical Research at the Department of Pathology and Laboratory Medicine, Detroit, MI, is thanked posthumously for mentoring (of G.E.B.) and supporting this work during its initial stages.

REFERENCES

1. Wind, T., Hansen, M., Jensen, J. K., and Andreasen, P. A. (2002) The molecular basis for anti-proteolytic and non-proteolytic functions of plasminogen activator inhibitor type-1: roles of the reactive centre loop, the shutter region, the flexible joint region and the small serpin fragment. *Biol. Chem. 383*, 21–36.
2. Durand, M. K., Bodker, J. S., Christensen, A., Dupont, D. M., Hansen, M., Jensen, J. K., Kjelgaard, S., Mathiasen, L., Pedersen, K. E., Skeldal, S., Wind, T., and Andreasen, P. A. (2004) Plasminogen activator inhibitor-I and tumour growth, invasion, and metastasis. *Thromb. Haemostasis 91*, 438–449.
3. Wiman, B. (1995) Plasminogen activator inhibitor 1 (PAI-1) in plasma: its role in thrombotic disease. *Thromb. Haemostasis 74*, 71–76.
4. Gettins, P. G. (2002) Serpin structure, mechanism, and function. *Chem. Rev. 102*, 4751–4804.
5. Irving, J. A., Pike, R. N., Lesk, A. M., and Whisstock, J. C. (2000) Phylogeny of the serpin superfamily: implications of patterns of amino acid conservation for structure and function. *Genome Res. 10*, 1845–1864.
6. Irving, J. A., Pike, R. N., Dai, W., Bromme, D., Worrall, D. M., Silverman, G. A., Coetzer, T. H., Dennison, C., Bottomley, S. P., and Whisstock, J. C. (2002) Evidence that serpin architecture intrinsically supports papain-like cysteine protease inhibition: engineering alpha(1)-antitrypsin to inhibit cathepsin proteases. *Biochemistry 41*, 4998–5004.
7. Silverman, G. A., Bird, P. I., Carrell, R. W., Church, F. C., Coughlin, P. B., Gettins, P. G., Irving, J. A., Lomas, D. A., Luke, C. J., Moyer, R. W., Pemberton, P. A., Remold-O'Donnell, E., Salvesen, G. S., Travis, J., and Whisstock, J. C. (2001) The serpins are an expanding superfamily of structurally similar but functionally diverse proteins. Evolution, mechanism of inhibition, novel functions, and a revised nomenclature. *J. Biol. Chem. 276*, 33293–33296.
8. Podor, T. J., Shaughnessy, S. G., Blackburn, M. N., and Peterson, C. B. (2000) New insights into the size and stoichiometry of the plasminogen activator inhibitor type-1·vitronectin complex. *J. Biol. Chem. 275*, 25402–25410.
9. Seiffert, D., Ciambrone, G., Wagner, N. V., Binder, B. R., and Loskutoff, D. J. (1994) The somatomedin B domain of vitronectin. Structural requirements for the binding and stabilization of active type 1 plasminogen activator inhibitor. *J. Biol. Chem. 269*, 2659–2666.
10. Deng, G., Royle, G., Seiffert, D., and Loskutoff, D. J. (1995) The PAI-1/vitronectin interaction: two cats in a bag? *Thromb. Haemostasis 74*, 66–70.
11. Lawrence, D. A., Olson, S. T., Palaniappan, S., and Ginsburg, D. (1994) Serpin reactive center loop mobility is required for inhibitor function but not for enzyme recognition. *J. Biol. Chem. 269*, 27657–27662.
12. Jensen, J. K., Wind, T., and Andreasen, P. A. (2002) The vitronectin binding area of plasminogen activator inhibitor-1, mapped by mutagenesis and protection against an inactivating organochemical ligand. *FEBS Lett. 521*, 91–94.
13. Zhou, A., Huntington, J. A., Pannu, N. S., Carrell, R. W., and Read, R. J. (2003) How vitronectin binds PAI-1 to modulate fibrinolysis and cell migration. *Nat. Struct. Biol. 10*, 541–544.
14. Lawrence, D. A., Berkenpas, M. B., Palaniappan, S., and Ginsburg, D. (1994) Localization of vitronectin binding domain in plasminogen activator inhibitor-1. *J. Biol. Chem. 269*, 15223–15228.
15. Podor, T. J., Peterson, C. B., Lawrence, D. A., Stefansson, S., Shaughnessy, S. G., Foulon, D. M., Butcher, M., and Weitz, J. I. (2000) Type 1 plasminogen activator inhibitor binds to fibrin via vitronectin. *J. Biol. Chem. 275*, 19788–19794.
16. Preissner, K. T., Grulich-Henn, J., Ehrlich, H. J., Declerck, P., Justus, C., Collen, D., Pannekoek, H., and Muller-Berghaus, G. (1990) Structural requirements for the extracellular interaction of plasminogen activator inhibitor 1 with endothelial cell matrix-associated vitronectin. *J. Biol. Chem. 265*, 18490–18498.
17. Rezaie, A. R. (1999) Role of exosites 1 and 2 in thrombin reaction with plasminogen activator inhibitor-1 in the absence and presence of cofactors. *Biochemistry 38*, 14592–14599.
18. Ehrlich, H. J., Gebbink, R. K., Keijer, J., Linders, M., Preissner, K. T., and Pannekoek, H. (1990) Alteration of serpin specificity by a protein cofactor. Vitronectin endows plasminogen activator inhibitor 1 with thrombin inhibitory properties. *J. Biol. Chem. 265*, 13029–13035.
19. Dupont, D. M., Madsen, J. B., Kristensen, T. K., Bødker, J. S., Wind, T., Blouse, G. E., and Andreasen, P. A. (2008) Biochemical properties of plasminogen activator inhibitor-1. *Front. Biosci.* (in press).
20. Preissner, K. T., and Seiffert, D. (1998) Role of vitronectin and its receptors in haemostasis and vascular remodeling. *Thromb. Res. 89*, 1–21.

[3] Personal communication from Michael Ploug, Daniel Hirschberg, and Thomas J. D. Jørgensen (Finsen Laboratory, Finsen Center, Rigshospitalet, and University of Southern Denmark).

21. Gebb, C., Hayman, E. G., Engvall, E., and Ruoslahti, E. (1986) Interaction of vitronectin with collagen. *J. Biol. Chem. 261*, 16698–16703.
22. Dufourcq, P., Louis, H., Moreau, C., Daret, D., Boisseau, M. R., Lamaziere, J. M., and Bonnet, J. (1998) Vitronectin expression and interaction with receptors in smooth muscle cells from human atheromatous plaque. *Arterioscler., Thromb., Vasc. Biol. 18*, 168–176.
23. Francois, P. P., Preissner, K. T., Herrmann, M., Haugland, R. P., Vaudaux, P., Lew, D. P., and Krause, K. H. (1999) Vitronectin interaction with glycosaminoglycans. Kinetics, structural determinants, and role in binding to endothelial cells. *J. Biol. Chem. 274*, 37611–37619.
24. Wei, Y., Waltz, D. A., Rao, N., Drummond, R. J., Rosenberg, S., and Chapman, H. A. (1994) Identification of the urokinase receptor as an adhesion receptor for vitronectin. *J. Biol. Chem. 269*, 32380–32388.
25. Huai, Q., Zhou, A., Lin, L., Mazar, A. P., Parry, G. C., Callahan, J., Shaw, D. E., Furie, B., Furie, B. C., and Huang, M. (2008) Crystal structures of two human vitronectin, urokinase and urokinase receptor complexes. *Nat. Struct. Mol. Biol. 15*, 422–423.
26. Andreasen, P. A., Egelund, R., and Petersen, H. H. (2000) The plasminogen activation system in tumor growth, invasion, and metastasis. *Cell. Mol. Life Sci. 57*, 25–40.
27. Peng, L., Bhatia, N., Parker, A. C., Zhu, Y., and Fay, W. P. (2002) Endogenous vitronectin and plasminogen activator inhibitor-1 promote neointima formation in murine carotid arteries. *Arterioscler., Thromb., Vasc. Biol. 22*, 934–939.
28. Podor, T. J., Joshua, P., Butcher, M., Seiffert, D., Loskutoff, D., and Gauldie, J. (1992) Accumulation of type 1 plasminogen activator inhibitor and vitronectin at sites of cellular necrosis and inflammation. *Ann. N.Y. Acad. Sci. 667*, 173–177.
29. Tomasini, B. R., Owen, M. C., Fenton, J. W., II, and Mosher, D. F. (1989) Conformational lability of vitronectin: induction of an antigenic change by alpha-thrombin-serpin complexes and by proteolytically modified thrombin. *Biochemistry 28*, 7617–7623.
30. Seiffert, D., and Loskutoff, D. J. (1996) Type 1 plasminogen activator inhibitor induces multimerization of plasma vitronectin. A suggested mechanism for the generation of the tissue form of vitronectin in vivo. *J. Biol. Chem. 271*, 29644–29651.
31. Seiffert, D., and Smith, J. W. (1997) The cell adhesion domain in plasma vitronectin is cryptic. *J. Biol. Chem. 272*, 13705–13710.
32. Gechtman, Z., Belleli, A., Lechpammer, S., and Shaltiel, S. (1997) The cluster of basic amino acids in vitronectin contributes to its binding of plasminogen activator inhibitor-1: evidence from thrombin-, elas. *Biochem. J. 325* (Part 2), 339–349.
33. Gechtman, Z., Sharma, R., Kreizman, T., Fridkin, M., and Shaltiel, S. (1993) Synthetic peptides derived from the sequence around the plasmin cleavage site in vitronectin. Use in mapping the PAI-1 binding site. *FEBS Lett. 315*, 293–297.
34. Kost, C., Stuber, W., Ehrlich, H. J., Pannekoek, H., and Preissner, K. T. (1992) Mapping of binding sites for heparin, plasminogen activator inhibitor-1, and plasminogen to vitronectin's heparin-binding region reveals a novel vitronectin-dependent feedback mechanism for the control of plasmin formation 1. *J. Biol. Chem. 267*, 12098–12105.
35. Minor, K. H., and Peterson, C. B. (2002) Plasminogen activator inhibitor type 1 promotes the self-association of vitronectin into complexes exhibiting altered incorporation into the extracellular matrix 1. *J. Biol. Chem. 277*, 10337–10345.
36. Minor, K. H., Schar, C. R., Blouse, G. E., Shore, J. D., Lawrence, D. A., Schuck, P., and Peterson, C. B. (2005) A mechanism for assembly of complexes of vitronectin and plasminogen activator inhibitor-1 from sedimentation velocity analysis. *J. Biol. Chem. 280*, 28711–28720.
37. Schar, C. R., Blouse, G. E., Minor, K. H., and Peterson, C. B. (2008) A deletion mutant of vitronectin lacking the somatomedin B domain exhibits residual PAI-1-binding activity. *J. Biol. Chem. 283*, 10297–10309.
38. Schar, C. R., Jensen, J. K., Andreasen, P. A., and Peterson, C. B. (2008) Characterization of a site on PAI-1 that binds to vitronectin outside the somatomedin B domain. *J. Biol. Chem. 283*, 28487–28496.
39. Andreasen, P. A., Riccio, A., Welinder, K. G., Douglas, R., Sartorio, R., Nielsen, L. S., Oppenheimer, C., Blasi, F., and Dano, K. (1986) Plasminogen activator inhibitor type-1: reactive center and amino-terminal heterogeneity determined by protein and cDNA sequencing. *FEBS Lett. 209*, 213–218.
40. Blouse, G. E., Perron, M. J., Thompson, J. H., Day, D. E., Link, C. A., and Shore, J. D. (2002) A concerted structural transition in the plasminogen activator inhibitor-1 mechanism of inhibition. *Biochemistry 41*, 11997–12009.
41. Kunkel, T. A., Bebenek, K., and McClary, J. (1991) Efficient site-directed mutagenesis using uracil-containing DNA. *Methods Enzymol. 204*, 125–139.
42. Kunkel, T. A., Roberts, J. D., and Zakour, R. A. (1987) Rapid and efficient site-specific mutagenesis without phenotypic selection. *Methods Enzymol. 154*, 367–382.
43. Ibarra, C. A., Blouse, G. E., Christian, T. D., and Shore, J. D. (2004) The contribution of the exosite residues of plasminogen activator inhibitor-1 to proteinase inhibition. *J. Biol. Chem. 279*, 3643–3650.
44. Wind, T., Jensen, J. K., Dupont, D. M., Kulig, P., and Andreasen, P. A. (2003) Mutational analysis of plasminogen activator inhibitor-1. *Eur. J. Biochem. 270*, 1680–1688.
45. Berkenpas, M. B., Lawrence, D. A., and Ginsburg, D. (1995) Molecular evolution of plasminogen activator inhibitor-1 functional stability. *EMBO J. 14*, 2969–2977.
46. Blouse, G. E., Perron, M. J., Kvassman, J. O., Yunus, S., Thompson, J. H., Betts, R. L., Lutter, L. C., and Shore, J. D. (2003) Mutation of the highly conserved tryptophan in the serpin breach region alters the inhibitory mechanism of plasminogen activator inhibitor-1. *Biochemistry 42*, 12260–12272.
47. Kvassman, J.-O., and Shore, J. D. (1995) Purification of human plasminogen activator inhibitor (PAI-1) from *Escherichia coli* and separation of its active and latent forms by hydrophobic interaction chromatography. *Fibrinolysis 9*, 215–221.
48. Shore, J. D., Day, D. E., Francis-Chmura, A. M., Verhamme, I., Kvassman, J., Lawrence, D. A., and Ginsburg, D. (1995) A fluorescent probe study of plasminogen activator inhibitor-1. Evidence for reactive center loop insertion and its role in the inhibitory mechanism. *J. Biol. Chem. 270*, 5395–5398.
49. Olson, S. T., Swanson, R., Day, D., Verhamme, I., Kvassman, J., and Shore, J. D. (2001) Resolution of Michaelis complex, acylation, and conformational change steps in the reactions of the serpin, plasminogen activator inhibitor-1, with tissue plasminogen activator and trypsin. *Biochemistry 40*, 11742–11756.
50. Backovic, M., Stratikos, E., Lawrence, D. A., and Gettins, P. G. (2002) Structural similarity of the covalent complexes formed between the serpin plasminogen activator inhibitor-1 and the arginine-specific proteinases trypsin, LMW u-PA, HMW u-PA, and t-PA: Use of site-specific fluorescent probes of local environment. *Protein Sci. 11*, 1182–1191.
51. Bradford, M. M. (1976) A rapid and sensitive method for the quantitation of microgram quantities of protein utilizing the principle of protein-dye binding. *Anal. Biochem. 72*, 248–254.
52. Perron, M. J., Blouse, G. E., and Shore, J. D. (2003) Distortion of the catalytic domain of tissue-type plasminogen activator by plasminogen activator inhibitor-1 coincides with the formation of stable serpin-proteinase complexes. *J. Biol. Chem. 278*, 48197–48203.
53. Gibson, A. D., Lamerdin, J. A., Zhuang, P., Baburaj, K., Serpersu, E. H., and Peterson, C. B. (1999) Orientation of heparin-binding sites in native vitronectin. Analyses of ligand binding to the primary glycosaminoglycan-binding site indicate that putative secondary sites are not functional. *J. Biol. Chem. 274*, 6432–6442.
54. Zhuang, P., Blackburn, M. N., and Peterson, C. B. (1996) Characterization of the denaturation and renaturation of human plasma vitronectin. I. Biophysical characterization of protein unfolding and multimerization. *J. Biol. Chem. 271*, 14323–14332.
55. Kjaergaard, M., Gardsvoll, H., Hirschberg, D., Nielbo, S., Mayasundari, A., Peterson, C. B., Jansson, A., Jorgensen, T. J., Poulsen, F. M., and Ploug, M. (2007) Solution structure of recombinant somatomedin B domain from vitronectin produced in *Pichia pastoris*. *Protein Sci. 16*, 1934–1945.
56. Mayasundari, A., Whittemore, N. A., Serpersu, E. H., and Peterson, C. B. (2004) The solution structure of the N-terminal domain of human vitronectin: proximal sites that regulate fibrinolysis and cell migration. *J. Biol. Chem. 279*, 29359–29366.
57. Jensen, J. K., Durand, M. K., Skeldal, S., Dupont, D. M., Bodker, J. S., Wind, T., and Andreasen, P. A. (2004) Construction of a plasminogen activator inhibitor-1 variant without measurable affinity to vitronectin but otherwise normal. *FEBS Lett. 556*, 175–179.
58. Kvassman, J. O., Verhamme, I., and Shore, J. D. (1998) Inhibitory mechanism of serpins: loop insertion forces acylation of plasmi-

nogen activator by plasminogen activator inhibitor-1. *Biochemistry 37*, 15491–15502.
59. Kirkegaard, T., Jensen, S., Schousboe, S. L., Petersen, H. H., Egelund, R., Andreasen, P. A., and Rodenburg, K. W. (1999) Engineering of conformations of plasminogen activator inhibitor-1. A crucial role of beta-strand 5A residues in the transition of active form to latent and substrate forms. *Eur. J. Biochem. 263*, 577–586.
60. Li, S. H., Gorlatova, N. V., Lawrence, D. A., and Schwartz, B. S. (2008) Structural differences between active forms of plasminogen activator inhibitor type 1 revealed by conformationally sensitive ligands. *J. Biol. Chem. 283*, 18147–18157.
61. Aleshkov, S. B., Fa, M., Karolin, J., Strandberg, L., Johansson, L. B., Wilczynska, M., and Ny, T. (1996) Biochemical and biophysical studies of reactive center cleaved plasminogen activator inhibitor type 1. The distance between P3 and P1′ determined by donor-donor fluorescence energy transfer. *J. Biol. Chem. 271*, 21231–21238.
62. Chang, A. W., Kuo, A., Barnathan, E. S., and Okada, S. S. (1998) Urokinase receptor-dependent upregulation of smooth muscle cell adhesion to vitronectin by urokinase. *Arterioscler., Thromb., Vasc. Biol. 18*, 1855–1860.
63. Ehrlich, H. J., Gebbink, R. K., Preissner, K. T., Keijer, J., Esmon, N. L., Mertens, K., and Pannekoek, H. (1991) Thrombin neutralizes plasminogen activator inhibitor 1 (PAI-1) that is complexed with vitronectin in the endothelial cell matrix. *J. Cell Biol. 115*, 1773–1781.
64. Park, Y.-J., Liu, G., Lorne, E. F., Zhao, X., Wang, J., Tsurata, Y., Zmijewski, J., and Abraham, E. (2008) PAI-1 acts as a "don't eat me signal", inhibiting neutrophil efferocytosis. *Proc. Natl. Acad. Sci. U.S.A.* (in press).
65. Aaboe, M., Offersen, B. V., Christensen, A., and Andreasen, P. A. (2003) Vitronectin in human breast carcinomas. *Biochim. Biophys. Acta 1638*, 72–82.
66. Kamikubo, Y., De Guzman, R., Kroon, G., Curriden, S., Neels, J. G., Churchill, M. J., Dawson, P., Oldziej, S., Jagielska, A., Scheraga, H. A., Loskutoff, D. J., and Dyson, H. J. (2004) Disulfide bonding arrangements in active forms of the somatomedin B domain of human vitronectin. *Biochemistry 43*, 6519–6534.
67. Deng, G., Royle, G., Wang, S., Crain, K., and Loskutoff, D. J. (1996) Structural and functional analysis of the plasminogen activator inhibitor-1 binding motif in the somatomedin B domain of vitronectin. *J. Biol. Chem. 271*, 12716–12723.
68. Mimuro, J., Muramatsu, S., Kurano, Y., Uchida, Y., Ikadai, H., Watanabe, S., and Sakata, Y. (1993) Identification of the plasminogen activator inhibitor-1 binding heptapeptide in vitronectin. *Biochemistry 32*, 2314–2320.
69. Wun, T. C., Palmier, M. O., Siegel, N. R., and Smith, C. E. (1989) Affinity purification of active plasminogen activator inhibitor-1 (PAI- 1) using immobilized anhydrourokinase. Demonstration of the binding, stabilization, and activation of PAI-1 by vitronectin. *J. Biol. Chem. 264*, 7862–7868.
70. Lindahl, T. L., Sigurdardottir, O., and Wiman, B. (1989) Stability of plasminogen activator inhibitor 1 (PAI-1). *Thromb. Haemostasis 62*, 748–751.
71. Fa, M., Karolin, J., Aleshkov, S., Strandberg, L., Johansson, L. B., and Ny, T. (1995) Time-resolved polarized fluorescence spectroscopy studies of plasminogen activator inhibitor type 1: conformational changes of the reactive center upon interactions with target proteases, vitronectin and heparin. *Biochemistry 34*, 13833–13840.
72. Gibson, A., Baburaj, K., Day, D. E., Verhamme, I., Shore, J. D., and Peterson, C. B. (1997) The use of fluorescent probes to characterize conformational changes in the interaction between vitronectin and plasminogen activator inhibitor-1. *J. Biol. Chem. 272*, 5112–5121.
73. Naski, M. C., Lawrence, D. A., Mosher, D. F., Podor, T. J., and Ginsburg, D. (1993) Kinetics of inactivation of alpha-thrombin by plasminogen activator inhibitor-1. Comparison of the effects of native and urea-treated forms of vitronectin. *J. Biol. Chem. 268*, 12367–12372.
74. Komissarov, A. A., Zhou, A., and Declerck, P. J. (2007) Modulation of serpin reaction through stabilization of transient intermediate by ligands bound to α helix F. *J. Biol. Chem. 282*, 26306–26315.
75. Komissarov, A. A., Andreasen, P. A., Bodker, J. S., Declerck, P. J., Anagli, J. Y., and Shore, J. D. (2005) Additivity in effects of vitronectin and monoclonal antibodies against α helix F of plasminogen activator inhibitor-1 on its reactions with target proteinases. *J. Biol. Chem. 280*, 1482–1489.
76. Lawrence, D. A., Palaniappan, S., Stefansson, S., Olson, S. T., Francis-Chmura, A. M., Shore, J. D., and Ginsburg, D. (1997) Characterization of the binding of different conformational forms of plasminogen activator inhibitor-1 to vitronectin. Implications for the regulation of pericellular proteolysis. *J. Biol. Chem. 272*, 7676–7680.

BI8017015